NWRI CONTRIBUTION 86-109

Lau (57)

ROUGHNESS OF REVERSE FLOW OVER DUNES AND ITS APPLICATION TO THE MODELLING OF THE PITT RIVER

by

Y.L. Lau

Environmental Hydraulics Section
Hydraulics Division
National Water Research Institute
Canada Centre for Inland Waters
Burlington, Ontario, Canada

June 1986

MANAGEMENT PERSPECTIVE

Computation of water levels in channel flow depends on knowing the roughness of the bottom. In the Fraser Estuary the flow reverses and because the bottom roughness in the form of dunes is not symmetrical, the same roughness does not apply for the ebb and flood tidal flows.

The report provides data in the bottom roughness for each flow direction. The data on the roughness for the reversed flow condition is not available elsewhere, but it is worth noting that the roughness for reversal flow is less than for the flow which formed the dunes.

T. Milne Dick
Chief
Hydraulics Division

ABSTRACT

Experiments using artificial dunes show that the friction factor is reduced when the steep face of the dune is on the upstream side, i.e., when the direction is reverse that of normal.

Calculations using bed-form regime relationships show that this configuration of reverse flow over dune profiles could have existed in the Pitt River, causing the decrease in bed roughness which was found during the calibration runs.

PERSPECTIVE GESTION

Pour calculer le niveau qui s'écoule dans un chenal, il faut connaître la rugosité du fond. Dans l'estuaire du Fraser, le sens du courant s'inverse en fonction de la marée. Or les dunes qui se forment sur le fond ne sont pas symétriques de sorte qu'elles n'offrent pas la même résistance à l'écoulement de l'eau selon que la marée monte ou descend.

Dans cette étude, on présente les données sur la rugosité du fond pour les deux sens d'écoulement du fleuve. Les données sur la rugosité du fond pour le courant inversé sont inédites. Soulignons que la rugosité dans ce sens est moindre que dans le sens du courant ayant formé les dunes.

Le chef, Division de l'hydraulique

T. Milne Dick

SOMMAIRE

Des expériences sur des dunes artificielles ont révélé qu'elles offrent moins de résistance à l'écoulement de l'eau lorsque le côté pentu est en amont, c'est-à-dire lorsque le profil de la dune est inversé par rapport à la normale.

D'après des calculs fondés sur les rapports fonctionnels entre la forme du lit et le régime d'écoulement d'une rivière, il semble qu'une situation analogue ait pu se produire dans la rivière Pitt (écoulement en sens inverse par rapport au profil des dunes), ce qui expliquerait que le fond de la rivière ait paru moins rugueux, comme on a pu le constater pendant les essais d'étalonnage.

1.0 INTRODUCTION

The Water Resources Branch of IWD is responsible for the sediment data collection program in the Lower Fraser River which provides input for the assessment of problems relating to navigation and other developments. The computation of the sediment discharge requires data on river discharge. Because of the difficulties encountered by the data collection program owing to tidal effects, a one-dimensional mathematical model was used to simulate the discharges in the Lower Fraser. This model was adapted and put into operation by the Planning and Management Branch, Ottawa, in cooperation with the Water Resources Branch.

During the calibration of the model, in which the Manning's roughness coefficient was adjusted until the simulated values of discharge and water surface elevation agreed with measured data, it was discovered that the discharge for the Pitt River section could not be simulated by using a constant value for the Manning's n. A value of n which correctly simulated the flood flow in the upstream direction from Port Mann to Port Coquitlam could not simulate the ebb flow in the downstream direction. A smaller value of Manning's n had to be used to simulate the ebb flow. The average value of n required for the flood period was 0.034 while that for the ebb period was 0.025. It was thought that the change in the roughness coefficient as the flow reversed was due to the presence of sand waves on the river bottom. The sand waves have a certain resistance to the flow in one direction but may present a different resistance when the flow direction reverses. The Hydraulics Division of the National Water Research Institute was requested to conduct a laboratory study to investigate the change in flow resistance so as to provide some guidance for the modelling and sampling programs.

2.0 EXPERIMENTAL PROCEDURE

In this study, artificial bedforms were used to simulate the dune roughness in a laboratory flume and the roughness coefficient was determined from several uniform flows. The bedforms were then removed and reinstalled in the opposite direction to simulate the roughness for reverse flow. The roughness coefficient for this configuration was again determined by setting up several uniform flows. Fig. 1 is a sketch of the test configurations. The normal flow direction is the one in which the long slope of the dunes is on the upstream side, the way sand wave would form in normal river flows.

Two sets of artificial dunes were fabricated from plywood. One set had a height, Δ, of 3 cm and a length, λ, of 150 cm while the other set had a height of 5.4 cm and a length of 90 cm. The downstream toe angle of the bedforms was 30°. The bedforms were the same width as the flume and covered nearly the whole of the flume length.

The flume was rectangular in cross section, 20 m long and 1 m wide. Dischages were measured at the downstream end using a weir box. Flow depths were measured using point gauges.

Each set of dunes was tested at two different flow depths. At each value of flow depth, several discharges were used so that there was a variation in average velocity and Froude number. The hydraulic variables are summarized in Tables 1 and 2.

3.0 RESULTS

Using the values of the discharge, Q, the flow depth h, and the slope of the uniform flow S, the Darcy-Weisbach friction factor, f, could be calculated. Because the side-walls of the flume were smooth, the side-wall correction procedure of Vanoni and Brooks (1957) was applied to obtain the friction factor for the bed, f_b. Knowing f_b, the hydraulic radius corresponding to the bed section, r_b, could be

calculated and the Manning's n for the bed section, n_b, could be obtained. These results are listed in Tables 1 and 2.

The data for f_b are plotted against the Froude number, F_r, in Fig. 2 and Fig. 3. In general, the friction factor seemed to be independent of the Froude number. This agrees with Engel and Lau (1980) who found that for rough turbulent flows at small Froude numbers, the bed form roughness is governed by the bed form steepness Δ/λ and the dimensionless bed form length λ/h.

For the normal flow direction, the values of f_b are much the same as those measured by Engel and Lau. For the steeper dunes, with $\Delta/\lambda = 0.06$, f_b values for $\lambda/h = 2\pi$ and $\lambda/h = 5$ average about 0.12 and 0.08 respectively. For $\Delta/\lambda = 0.02$, f_b values for $\lambda/h = 10$ and $\lambda/h = 2\pi$ are about 0.05 and 0.04 respectively. These f_b values can also be compared with the roughness calculated from a method proposed by van Rijn (1984) who obtained an empirical expression for the equivalent roughness on bed forms based on a large amount of flume and field data. van Rijn's expression for the form roughness, $k_{s,form}$, is

$$k_{s,form} = 1.1\Delta(1 - e^{-25\Delta/\lambda}) \qquad (1)$$

The Chezy-coefficient, C, can be computed from

$$C = 18 \log \left(\frac{12\, r_b}{k_s}\right) \qquad (2)$$

The friction factor is then given by

$$f = \frac{8g}{C^2} \qquad (3)$$

The friction factor values for the bed forms tested were calculated using this method and are also tabulated in Tables 1 and 2.

It can be seen that the values compare fairly well with the present experimental data.

When the dunes are reversed, the experimental data show that the friction factor is reduced. From Figs. 2 and 3 it can be seen that this reduction occured for each of the two flow depths for both sets of dunes. For $\Delta/\lambda = 0.02$, the f_b values are roughly equal to 0.02. For $\Delta/\lambda = 0.06$, f_b values are about 0.07 and 0.05 for $\lambda/h = 2\pi$ and $\lambda/h = 5$ respectively. This may be slightly unexpected because one tends to get the impression that, in the reverse flow situation, the water is flowing against the steeper face, opposite to the direction in which sand waves are formed and the resistance would increase as a consequence. However, on closer scrutiny, one can see that such is not the case. The energy loss in the flow over these bed forms consists mainly of the form loss due to the separation of the flow over the crest of the dunes. The flow cannot follow the rapid divergence of the boundary, resulting in the separation and the creation of an eddy region just downstream of the crest. In the reverse flow situation the flow experiences a rapid convergence and then a very gradual divergence much like the flow in a Venturi meter. The tendency for flow separation is greatly reduced. Flow visualization using dye confirmed that there was indeed very little separation. Therefore, one should expect the energy loss to be smaller when the flow is in the reverse direction, as indicated by the present experiment data.

4.0 FLOW RESISTANCE IN THE PITT RIVER

Having established that the flow resistance of the artificial dunes decreases when the flow is in the reverse direction, one can try to apply this finding to the Pitt River situation. In order to do so, it is necessary to decide whether the reverse flow configuration had actually occurred during either the flood flow or ebb flow periods. Therefore, one has to try and estimate the sand wave properties which existed during the calibration runs and create a picture of the bed form

characteristics during the tidal cycle. The bed form regime can be estimated using the method proposed by van Rijn (1984).

van Rijn characterized the generation of bed forms using two variables - a dimensionless particle diameter and a transport stage parameter which is related to the grain shear stress. Using a large number of flume and field data he showed that there were distinct zones for the existence of the various bed forms on a plot of the transport stage parameter against dimensionless particle diameter. This plot is reproduced in Fig. 4. Therefore by evaluating these two parameters for the periods of the calibration runs one can establish the type of bed forms that could have existed during these periods.

The dimensionless particle diameter, D_*, is defined as

$$D_* = D_{50} \left[\frac{(s - 1)g}{\nu^2} \right]^{1/3} \qquad (4)$$

in which D_{50} = mean diameter of bed material; s = specific density of the material; g = gravitational acceleration and ν = kinematic viscosity.

Based on a study by Ashley (1977) who found that the mean grain size of the sediments decreased from 0.37 mm at the downstream end near the Pitt-Fraser confluence to 0.25 mm at the upstream end at Pitt Lake, the values of D_{50} and D_{90} for the Port Coquitlam section was taken to be 0.33 mm and 1.20 mm respectively. Assuming a water temperature of about 7°C for the November period, the value of D_* is 6.6.

The transport stage parameter, T, is defined as

$$T = \frac{U_*'^2 - U_{*cr}^2}{U_{*cr}^2} \qquad (5)$$

in which $U_*' = (g^{0.5}/C')\,\bar{U}$ = bed shear velocity related to grain roughness; C' = Chézy coefficient related to grains = 18 log $(12r/3D_{90})$; r = hydraulic radius; $\bar{U}$ = mean flow velocity; and $U_{*_{cr}}$ = critical bed shear velocity. For the 0.33 mm sand; $U_{*_{cr}}$ = 1.35 cm/s.

Using the values of mean velocity and hydraulic radius provided by the calibration run of the mathematical model, the values of T were calculated for various times in the tidal cycle and are listed in Table 3. From the plot given by van Rijn (1984) the bed form regime for those flow conditions are noted. It can be seen from Table 3 that only the conditions at or near maximum flood flow were strong enough for the bed forms to be in the dune regime. During the period of changeover from one flow direction to the other there will be no sediment movement. For the rest of the time, the flow could only create ripples.

Based on the above information one can make an informed estimate of the bed form developments during the tidal cycle. As the flow reaches the maximum flood flow, dunes are formed. The discharge then decreases and the flow falls into the range where only ripples can be formed. During this period, one may find ripples superimposed on top of the dune profile. The discharge continues to decrease and this pattern stays until the flow reverses and the ebb flow becomes strong enough to initiate sediment movement. During the ebb cycle the ripples are modified so that they point in the downstream direction. However, the dune profile formed during the flood flow still remains, although the dune crest may get slightly rounded. This pattern remains until flood flow returns, with ripples and then dunes as before. Thus the dune profiles formed during the high flood flow persist throughout the whole tidal cycle, with ripples superimposed on them at various times. The picture of the bottom profile should appear more or less as shown in Fig. 5. It is interesting to note that the echo sounding survey conducted by Ashley (1977) found large scale sand waves, the majority of which have small scale sand waves superimposed on their long slopes.

The above picture of the bed profile development indicates that there will be a difference in the flow resistance between the flood

flow and ebb flow periods. In both cases the form loss created by the dune profile governs the flow resistance. During the flood cycle the flow resistance is provided mainly by the dune profiles in the normal flow direction. The ripples which are superimposed on the dune profiles behave like roughness elements on the dune surface and this will increase the overall roughness slightly (Engel and Lau, 1980). During the ebb cycle, one gets the reverse flow configuration over the same dune profile, again with ripples superimposed. The present experiments show that this configuration will offer less resistance.

Some calculations can be made to see if the change in bed profile configuration described here can be responsible for the change in flow resistance required by the mathematical model. The following empirical relationships obtained by van Rijn (1984) can be used to calculate the roughness

$$\frac{\Delta}{\lambda} = 0.015 \left(\frac{D_{50}}{h}\right)^{0.3} (1 - e^{-.5T}) (25 - T) \qquad (6)$$

and

$$k_s = 3D_{90} + 1.1\,\Delta(1 - e^{-25\Delta/\lambda}) \qquad (7)$$

in which k_s = equivalent sand grain roughness.

Using the value of $T = 3.2$ from Table 3 for maximum flood flow, Eq. (6) gives the dune steepness $\Delta/\lambda = 0.014$. The dune length has been shown to be related only to the flow depth (Yalin, 1972; van Rijn, 1984). Based on the relationship given by van Rijn, $\lambda = 7.3$ h. This gives a dunes length of 45.4 m and a dune height of 0.65 m. These should, of course, be considered as average values only as there is a fair amount of scatter in the data from which the empirical relationships were derived. Using these values $k_s = 0.21$ m. The Chézy coefficient, C, is given by

$$C = 18 \log \left(\frac{12\,r}{k_s}\right) = 45.86 \frac{m^{1/2}}{s} \qquad (8)$$

Therefore

$$n = \frac{r^{1/6}}{C} = 0.03 \qquad (9)$$

During the ebb flow period, the flow resistance has to be estimated from the experimental data obtained in this study because there are no other data on flow in the reverse direction over dunes.

From Fig. 3 it can be seen that for $\Delta/\lambda = .02$, the Darcy Weisbach friction factor is approximatley equal to 0.02. This value may be slightly on the high side because the dune steepness for the Pitt is estimated to be only .014. Based on this value of f, and an averge value of r of 18.8 ft for the ebb flow period,

$$n = \left(\frac{f}{8g}\right)^{1/2} r^{1/6} = 0.02$$

Thus, using the estimated sand wave properties for the tidal cycle, a decrease in Manning's n from .03 for flood flow to .02 for ebb flow is predicted. These values cannot be directly compared with those used in the calibration of the mathematical model because the Manning's values used in the mathematical model had been increased to make allowance for the resistance of log covers on the water surface. However, these values are close enough to give confidence to the picture of the bed profile described above and to show that there is a decrease in the flow resistance during the ebb cycle because the flow is going in the reverse direction over the dune profiles which are formed during the flood cycle.

5.0 SUMMARY AND CONCLUSIONS

In flows having sand waves on the channel bed, the sand waves, in their usual orientation, create a certain resistance to the flow. When the flow reverses its direction, the present experiments show that, if the bed form profiles remain unchanged, the flow resistance will be decreased.

For the flow conditons in the Pitt River which were found during the calibration of the mathematical model, it can be shown using

bed form regime relationships that, during the ebb flow period, the flow is likely going in the reverse direction over the dunes which were formed during the flood flow period. Calculations using empirical bed form and resistance equations and the present data on reverse flow give a change in Manning's n similar to what was found from the calibration runs. Therefore, the reverse flow over dunes is probably responsible for the change in flow resistance between the flood and ebb flow periods.

This study points out the need to pay close attention to the relationship between the flow and the bed when modelling tidal rivers with sand beds such as the Pitt-Fraser system. The modeller has to take into account the changes in bed form regime as flow conditions change. Moreover, the flow conditions over the whole tidal cycle has to be looked at. In the present example, the flow resistance is obviously controlled by the dune bed profile even though the flow conditions during most of the tidal cycle is in the range where only ripples would exist if the flow were uni-directional and steady.

The relationship used in this study were derived from steady flow experiments. This may not always be reliable when dealing with unsteady flows. It is known that a lag exists between changes in flow conditions and changes in bed configuration (Allen, 1973; Simons et al. 1962; Wijbenga and Klaasen, 1986). Two different sizes of bed forms can occur for the same discharge and same flow depth at the rising and falling stages of a flood. The manner in which the flow changes has a very important effect. If the flow decreases very rapidly, the dunes which were formed may remain intact and one may have dunes existing in a flow which is not even strong enough to initiate sediment movement. If the same flow decreases very gradually, the dunes may be altered significantly. In short, the history of the flow exerts an influence on the bedforms. This is further complicated by reversing flow in tidal situations. Quantitative information on the response of sand beds to flow variations is very scarce. Such information will certainly be required so that modelling of the Fraser or other similar rivers can be carried out successfully.

ACKNOWLEDGEMENTS

The author would like to thank M. Sydor, Water Planning and Management Branch and B. Tassone, Water Resources Branch for providing the background material and the data from the calibration runs.

REFERENCES

Allen, J.R.L. 1973. Phase Differences Between Bed Configuration and Flow in Natural Environments, and Their Geological Relevance. Sedimentology, Vol. 20, pp. 323-329.

Ashley, G.M. 1977. Sedimentology of a Freshwater Tidal System, Pitt River - Pitt Lake, British Columbia. Thesis submitted in partial fulfilment of the requirements for the degree of Doctor of Philosophy, University of British Columbia.

Engel, P. and Y.L. Lau. 1980. Friction Factor for Two-Dimensional Dune Roughness. Journal of the International Association of Hydraulic Research, Vol. 18, No. 3.

Inland Waters Directorate. 1983. The Applicaion of a 1-Dimensional Hydrodynamic Model to the Lower Fraser River. Report prepared by the Water Planning and Management Branch and Water Resources Branch, Environment Canada, Ottawa.

Simons, D.B., E.V. Richardson and W.L. Haushild. 1962. Depth-Discharge Relations in Alluvial Streams. Proc. Am. Soc. Civ. Engrs., Vol. 88, YT5, pop. 57-72.

Vanoni, V.A. and N.H. Brooks. 1957. Laboratory Studies of the Roughness and Suspended Load of Alluvial Streams. Report E-68, Sedimentation Laboratory, Calif. Inst. of Techn., Pasadena, Calif.

van Rijn, L.C. 1984. Sediment Transport, Part III: Bed Forms and Alluvial Roughness. Journal of Hydraulic Engineering, ASCE, Vol. 110, No. 12, pp. 1733-1754.

Wijbenga, J.H.A. and Klaassen, G.J. 1981. Changes in Bedform Dimensions under Unsteady Flow Conditions in a Straight Flume. Publication No. 20, Delft Hydrauics Laboratory, Delft.

Yalin, M.S. 1972. Mechanics of Sediment Transport. Pergamon Press.

TABLE 1. Hydraulic Variables and Results for Dune with λ = 90 cm, Δ = 5.4 cm; Δ/λ = .06

Flow Direction	h cm	Q m^3/s	U m/s	S	F_r	f_b	n_b	f*
normal	14.3	.0294	.205	.00045	.17	.114	.027	.101
"	"	.0360	.252	.00062	.21	.103	.026	.102
"	"	.0494	.307	.00102	.26	.114	.027	.102
"	"	.0534	.374	.00166	.32	.127	.029	.101
"	"	.0620	.433	.00239	.37	.135	.030	.101
"	"	.0221	.154	.00028	.09	.123	.028	.102
"	"	.0364	.255	.00065	.21	.105	.026	.102
reversed	"	.0289	.202	.00030	.17	.076	.022	NA
"	"	.0362	.253	.00041	.21	.066	.021	NA
"	"	.0474	.330	.00073	.28	.069	.021	NA
"	"	.0576	.403	.00110	.34	.070	.021	NA
"	"	.0213	.149	.00015	.13	.069	.021	NA
normal	18.0	.0360	.200	.00025	.15	.80	.024	.091
"	"	.0418	.232	.00033	.18	.079	.021	.091
"	"	.0539	.300	.00064	.23	.092	.025	.091
"	"	.0646	.359	.00092	.27	.093	.026	.091
"	"	.0234	.130	.00009	.10	.066	.021	.093
"	"	.0300	.167	.00017	.13	.077	.023	.092
reversed	"	.0350	.193	.00015	.15	.050	.019	NA
"	"	.0455	.253	.00021	.19	.039	.016	NA
"	"	.0539	.300	.00041	.23	.058	.020	NA
"	"	.0653	.363	.0060	.27	.057	.020	NA
"	"	.0790	.437	.00090	.33	.060	.020	NA

* Evaluated using equations (1) to (3)

TABLE 2. Hydraulic Variables and Results for Dune with λ = 150 cm, Δ = 3 cm; Δ/λ = .02

Flow Direction	h cm	Q m^3/s	U m/s	S	F_r	f_b	n_b	f*
normal	15.0	.0451	.301	.00050	.25	.059	.020	.055
"	"	.0600	.400	.00071	.33	.046	.017	.056
"	"	.0696	.464	.00085	.38	.041	.016	.055
"	"	.0798	.532	.00110	.44	.040	.016	.055
"	"	.0913	.609	.00143	.50	.040	016	.055
"	"	.0301	.209	.00022	.17	.057	.019	.055
"	"	.0358	.239	.00026	.20	.047	.017	.056
"	"	.0419	.279	.00033	.23	.044	.017	.056
"	"	.0479	.319	.00047	.26	.049	.018	.055
"	"	.0475	.317	.00040	.26	.041	.016	.055
"	"	.0608	.405	.00066	.33	.041	.016	.056
reversed	"	.0345	.230	.00011	.19	.019	.011	NA
"	"	.0496	.331	.00025	.27	.021	.012	NA
"	"	.0640	.427	.00052	.35	.029	.014	NA
"	"	.0440	.293	.00018	.24	.020	.011	NA
"	"	.0551	.367	.00034	.30	.025	.013	NA
normal	23.9	.0733	.307	.00030	.20	.050	.019	.047
"	"	.0798	.334	.00038	.22	.052	.019	.048
"	"	.0959	.401	.00046	.23	.045	.018	.047
"	"	.1215	.508	.00061	.33	.037	.016	.048
"	"	.1376	.576	.00073	.38	.034	.016	.048
"	"	.1590	.665	.00091	.43	.031	.015	.048
"	"	.0608	.254	.00021	.17	.052	.020	.047
"	"	.0759	.318	.00025	.21	.038	.017	.048
reversed	"	.0498	.208	.00005	.14	.015	.010	NA
"	"	.0710	.297	.00011	.19	.016	.011	NA
"	"	.0818	.342	.00016	.22	.018	.010	NA
"	"	.0948	.397	.00026	.26	.024	.013	NA
"	"	.1137	.476	.00040	.31	.025	.014	NA

* Evaluated using equations (1) to (3)

TABLE 3. Hydraulic Data from Mathematical Model Output and the Calculated Transport Stage Parameter

Date	Time hr	Flow Direction	Discharge ft /s	U ft/s	r ft.	T	Bedform
Nov. 15/80	11	flood	61,773	1.81	19.71	1.74	ripples
"	12	"	75,676	2.14	20.13	2.80	"
"	13	"	82,078	2.25	20.41	3.20	dunes
"	15	"	62,678	1.74	20.25	1.52	ripples
"	16	"	40,349	1.16	19.95	0.12	"
"	17	"	13,078	0.39	19.62	-	No movement
Nov. 16/80	6	ebb	51,743	1.78	18.84	1.66	ripples
	7	"	51,869	1.80	18.71	1.66	"
	8	"	42,613	1.49	18.68	0.78	"
	9	"	22,809	0.78	18.88	-	"

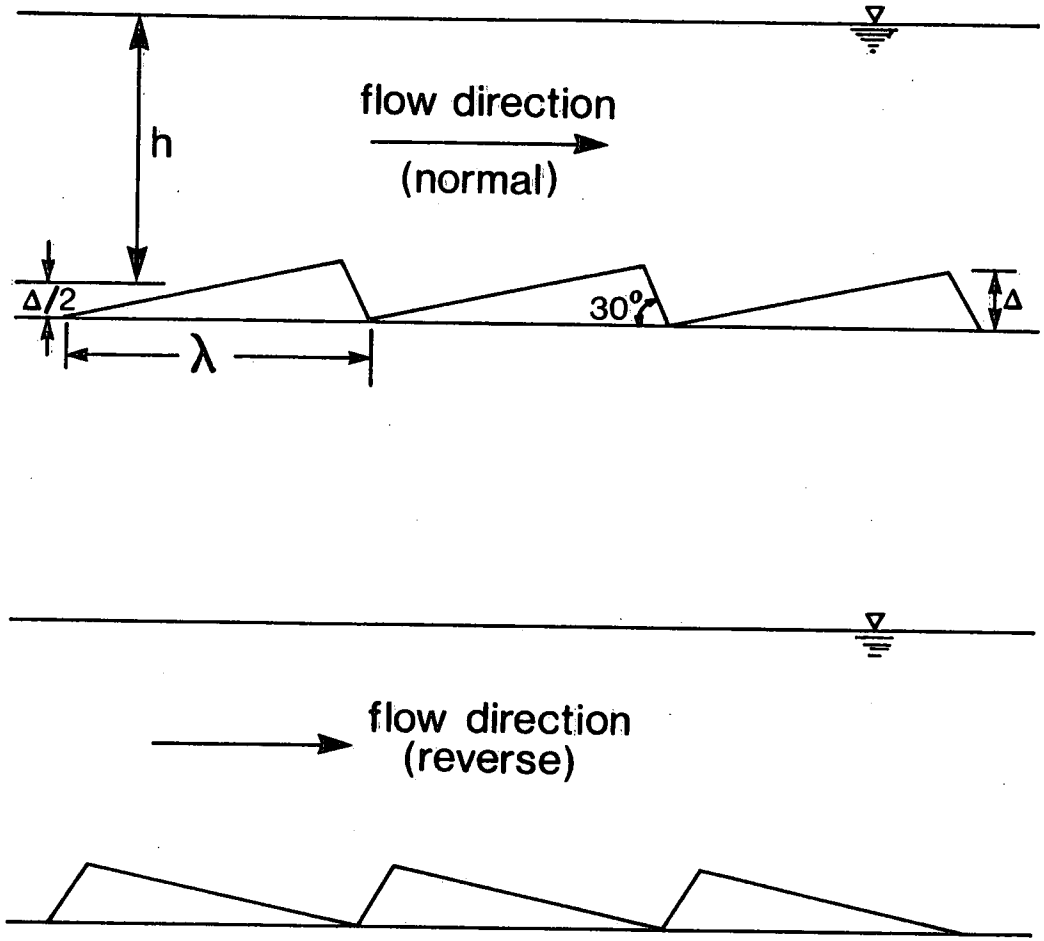

FIGURE 1. SKETCH OF TEST CONFIGURATIONS WITH ARTIFICIAL DUNES

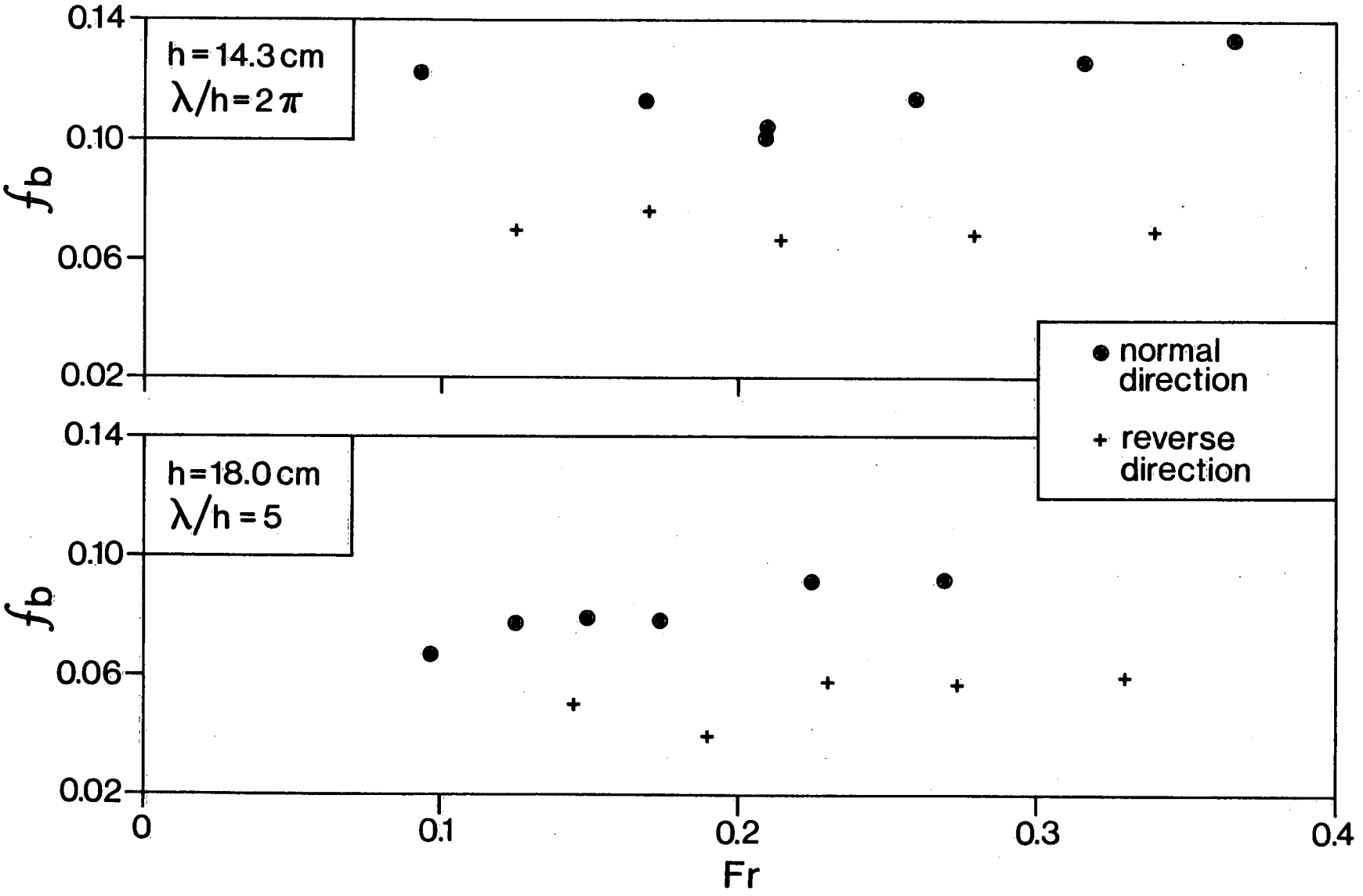

FIGURE 2. BED FRICTION FACTOR VERSUS FROUDE NUMBER FOR $\Delta/\lambda = 0.06$

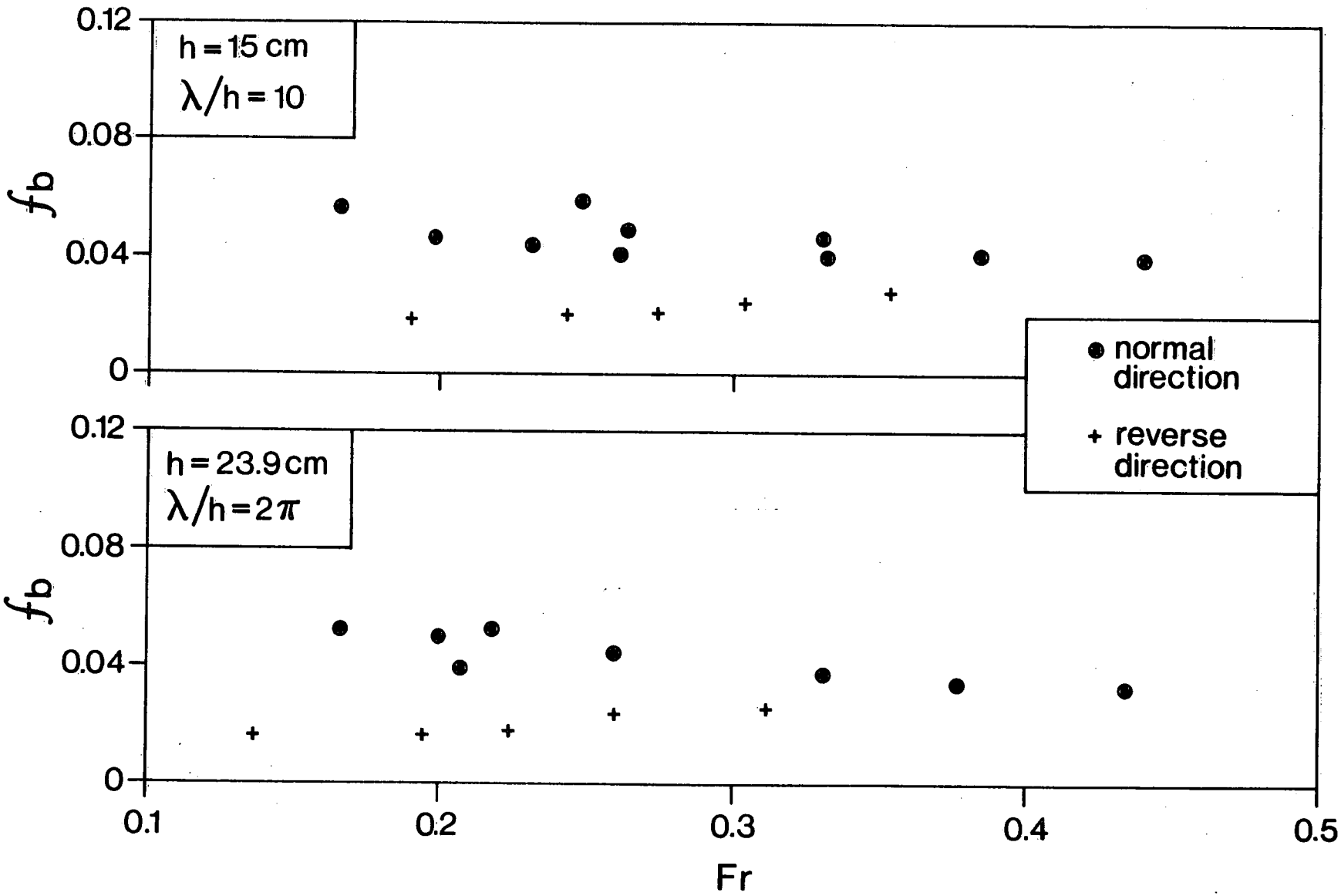

FIGURE 3. BED FRICTION FACTOR VERSUS FROUDE NUMBER FOR $\Delta/\lambda = 0.02$

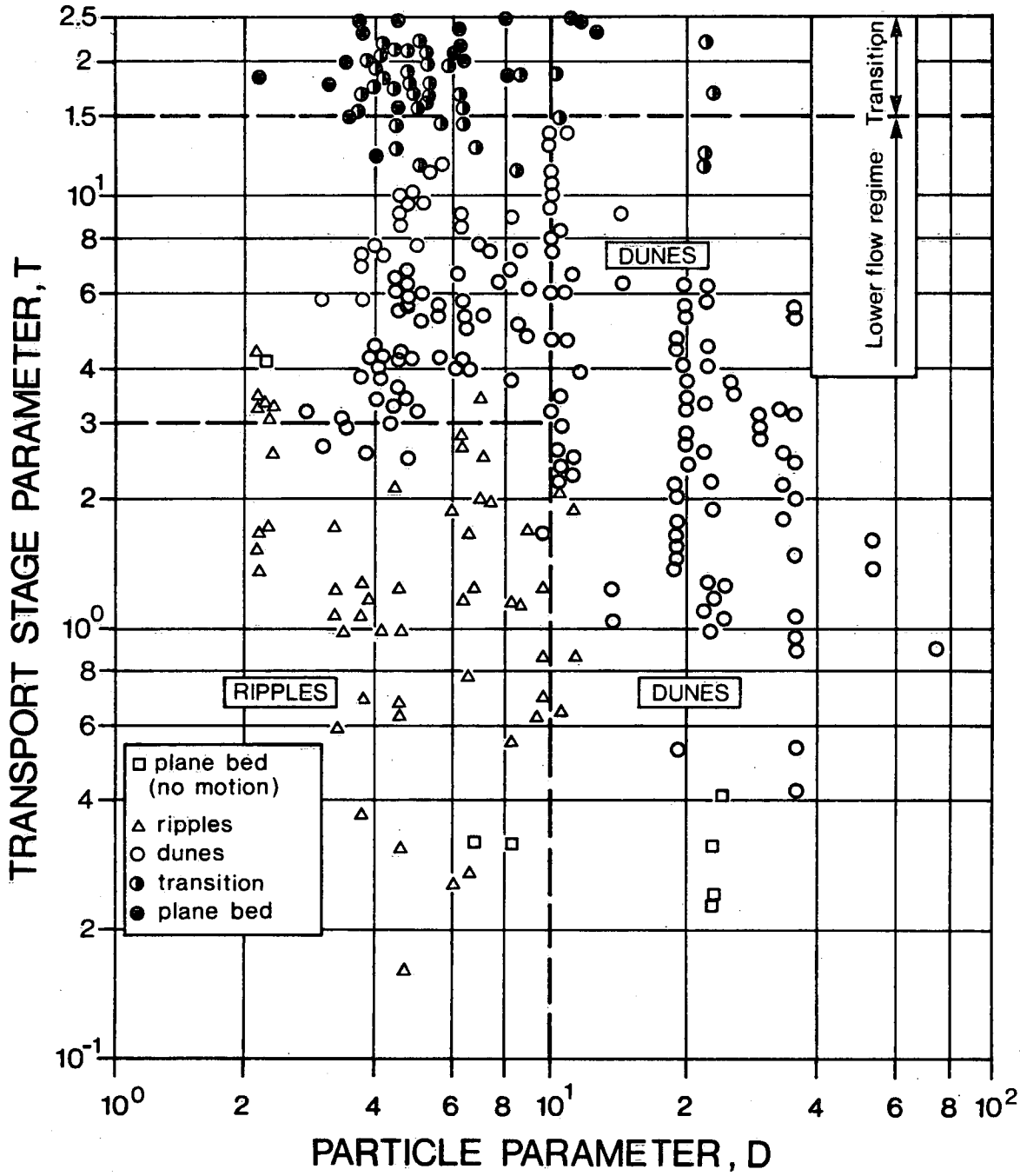

FIGURE 4. DIAGRAM FOR BED FORM CLASSIFICATION (from van Rijn, 1984)

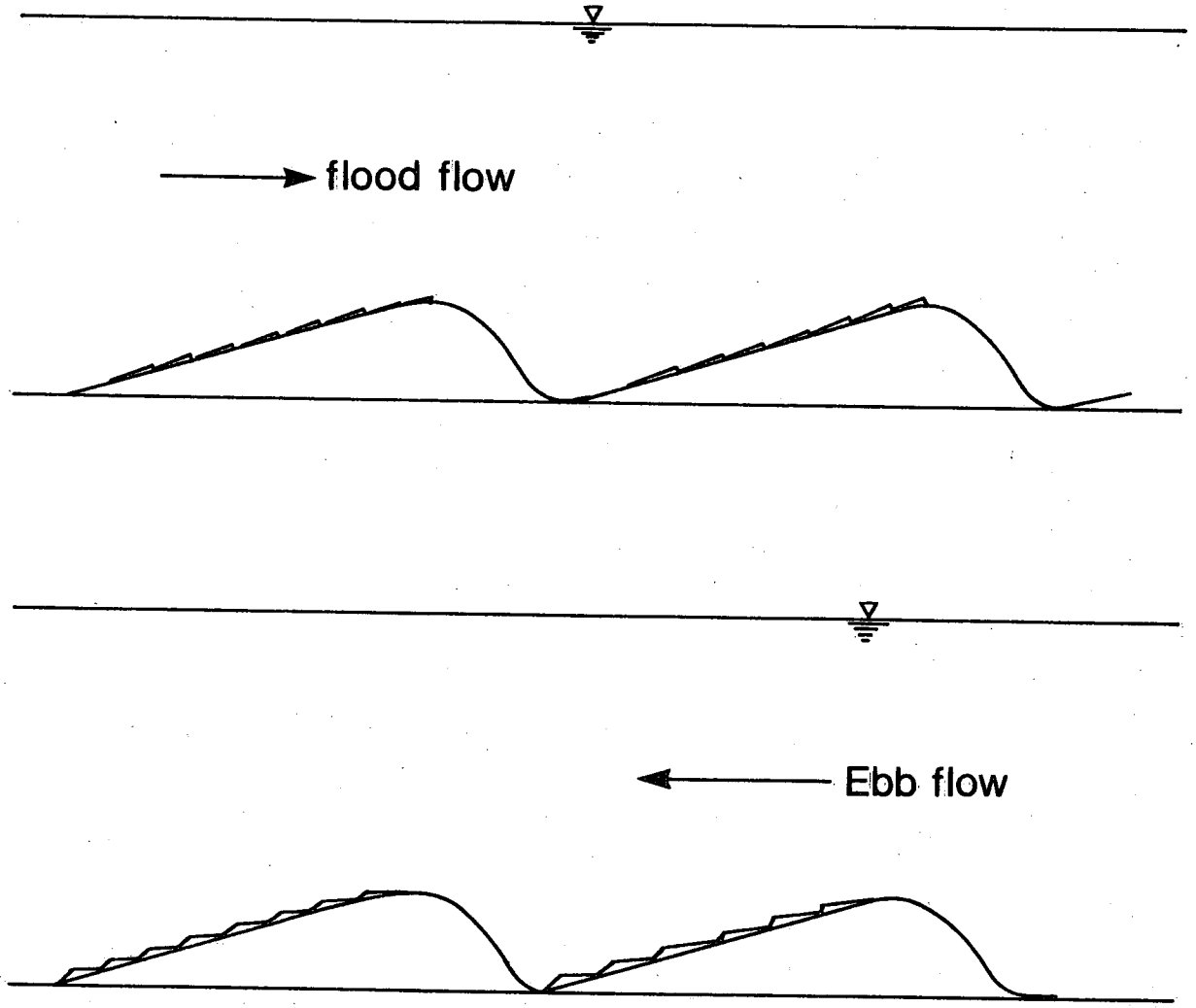

FIGURE 5. PROBABLE BED CONFIGURATIONS